

A Method to Estimate the Probability that any Individual Cloud-to-Ground Lightning Stroke was within any Radius of any Point

Lisa L. Huddleston
NASA, Kennedy Space Center, Florida

William P. Roeder
45th Weather Squadron, Patrick AFB, Florida

Francis J. Merceret
NASA, Kennedy Space Center, Florida

Corresponding author address: Lisa L. Huddleston, NASA, Mail Code: NE-M5, Kennedy Space Center
FL 32899.
E-mail: lisa.l.huddleston@nasa.gov, 321-861-4952

Abstract

A new technique has been developed to estimate the probability that a nearby cloud-to-ground lightning stroke was within a specified radius of any point of interest. This process uses the bivariate Gaussian distribution of probability density provided by the current lightning location error ellipse for the most likely location of a lightning stroke and integrates it to determine the probability that the stroke is inside any specified radius of any location, even if that location is not centered on or even within the location error ellipse. This technique is adapted from a method of calculating the probability of debris collision with spacecraft. Such a technique is important in spaceport processing activities because it allows engineers to quantify the risk of induced current damage to critical electronics due to nearby lightning strokes. This technique was tested extensively and is now in use by space launch organizations at Kennedy Space Center and Cape Canaveral Air Force station. Future applications could include forensic meteorology.

1. Introduction

The ability to accurately estimate the probability that an individual nearby cloud-to-ground lightning stroke was within a specified distance of any specified spaceport processing facility at Kennedy Space Center (KSC) or Cape Canaveral Air Force Station (CCAFS) is important to processing payloads and space launch vehicles before launch. Such estimates allow engineers to decide if inspection of electronics systems aboard satellite payloads, space launch vehicles, and ground support equipment is warranted due to induced currents from that stroke. If induced current damage has occurred, inspections of the electronics are critical to identify required fixes and avoid degraded performance or failure of the satellite or space launch vehicle. However, inspections are costly both financially and in terms of delayed processing for space launch activities. As such, it is important these inspections be avoided if not needed. At KSC/CCAFS, one of the main purposes of the Four Dimensional Lightning Surveillance System (4DLSS) (Murphy et al 2008, Roeder 2010) is detection of nearby strokes and determination of their peak current to support electronics inspection decisions (Flinn et al 2010a, Flinn et al 2010b, Roeder et al 2005). The high frequency of lightning occurrence in East Central Florida combined with the large amount of complex sensitive electronics in satellite payloads, space launch vehicles, and associated facilities makes those decisions critically important to space launch processing. The 4DLSS provides the data for 50th percentile location error ellipses for the best location for each stroke, which is then scaled to 95th or 99th percentile ellipses depending on customer requirements. However, 4DLSS has not been able to provide the probability of the stroke being within a customer specified distance of

a point of interest. This paper presents a new method to convert the 4DLSS 50th percentile location error ellipse for best location of any stroke into the probability that the stroke was within any radius of any facility at CCAFS/KSC. It may also be used with National Lightning Detection Network (NLDN) data at any location where the NLDN is available. This new facility-centric technique is a significant improvement over the stroke-centric location error ellipses the 45th Weather Squadron (45WS) has provided in the past. This technique is adapted from a method of calculating the probability of debris collision with spacecraft (Chan 2008, Leleux 2002, Patera 2001).

2. Methodology

a. Background

In spacecraft collision probability and other applications, at the instant of “nominal” closest approach, the position uncertainty of the collision object relative to the asset being protected is described by a bivariate Gaussian probability density function (pdf) (Alfano 2007, Alfano 2009, Chan 2008, Patera 2001), as shown in the following equation.

$$f(x, z) = \frac{1}{2\pi\sigma_x\sigma_z\sqrt{1-\rho_{xz}^2}} e^{-\left[\left(\frac{x}{\sigma_x}\right)^2 - 2\rho_{xz}\left(\frac{x}{\sigma_x}\right)\left(\frac{z}{\sigma_z}\right) + \left(\frac{z}{\sigma_z}\right)^2\right]/2(1-\rho_{xz}^2)} \quad (1)$$

where σ_x and σ_z = the standard deviations of x and z , ρ_{xz} = correlation coefficient of x and z , x and z are the designations for the rectangular coordinates in the collision plane.

The probability of collision (equation (2)) is given by the two-dimensional integral, where A is the collision cross-sectional area which is a circle with radius, r_A (Chan 2008).

$$P = \iint_A f(x, z) dx dz \quad (2)$$

There is no known analytical solution to the above integral when the two standard deviations σ_x and σ_z are not equal. The solution is found by performing a numerical integration of the two dimensional Gaussian pdf (Alfano 2007, Alfano 2009, Chan 2008, Patera 2001).

The geometry used for spaceflight collision probability can also be used for estimation of the probability of an individual nearby lightning stroke contacting the surface within a specified distance of a specified point of interest as shown in Figure 1. Both solution methods are based on algorithms by Patera (2001) as implemented by Chan (2009, private communication) and Chan, 2011 will be evaluated in the next section.

b. The first numerical integration technique (Patera, 2001)

This numerical integration technique is an algorithm that solves the probability of collision, equation (2), by converting the position uncertainty equation described by a bivariate Gaussian pdf (equation (1)) into a probability circle and the target area of interest into an ellipse. The area of the ellipse is integrated numerically by reducing the two-dimensional integral to a one-dimensional integral involving a simple exponential function in the integrand (Patera 2001, Chan 2009 personal communication). The following equations, from Chan 2008 and Patera 2001 as implemented by Chan (2009, private communication), outline the algorithm. Any changes in terminology due to differences in spacecraft collision vs. lightning strike probability are annotated.

The covariance matrix corresponding to the bivariate Gaussian pdf in equation (1) is (Chan 2008):

$$C = \begin{bmatrix} \sigma_x^2 & \rho_{xz} \sigma_x \sigma_z \\ \rho_{xz} \sigma_x \sigma_z & \sigma_z^2 \end{bmatrix} \quad (3)$$

When the correlation coefficient, ρ_{xz} , is not zero, there are undesirable off-diagonal terms. In order to eliminate these terms, the coordinate system (x,z) is rotated to a new coordinate system (x',z') such that the major and minor axes of the ellipse associated with the covariance are aligned along the coordinate axes and the new covariance matrix is (Chan 2008):

$$C' = \begin{bmatrix} \sigma_{x'}^2 & 0 \\ 0 & \sigma_{z'}^2 \end{bmatrix} \quad (4)$$

The angle, θ , between the two coordinate systems is (Chan 2008):

$$\theta = \frac{1}{2} \tan^{-1} \left[\frac{2\rho_{xz} \sigma_x \sigma_z}{(\sigma_x^2 - \sigma_z^2)} \right] \quad (5)$$

The KSC/CCAFS 4DLSS system does not provide the covariance matrix, but instead provides the semi-major axis, semi-minor axis, and the orientation of the semi-major axis of the 50% location error ellipse relative to north. Therefore the angle, θ , in equation (5) is found using geometry where θ is the angle between the semi-major axis of the lightning location uncertainty ellipse and line connecting the center of the lightning uncertainty ellipse and the center of the area of interest.

In the (x', z') system, the equation (1) pdf becomes (Chan 2008)

$$f(x', z') = \frac{1}{2\pi\sigma_{x'}\sigma_{z'}} e^{-\frac{1}{2}\left[\left(\frac{x'}{\sigma_{x'}}\right)^2 + \left(\frac{z'}{\sigma_{z'}}\right)^2\right]} \quad (6)$$

and equation (2), the collision probability becomes (Chan 2008)

$$P = \frac{1}{2\pi\sigma_{x'}\sigma_{z'}} \iint_{A'} e^{-\frac{1}{2}\left[\left(\frac{x'}{\sigma_{x'}}\right)^2 + \left(\frac{z'}{\sigma_{z'}}\right)^2\right]} dx' dz' \quad (7)$$

where

$$A' = A, r_{A'} = r_A, x'_p = x_e \cos \theta, z'_p = x_e \sin \theta \quad (8)$$

For spacecraft collision, x_e is the nominal distance of closest approach of the two colliding objects and (x'_p, z'_p) are the coordinates of the spacecraft relative to the debris. For lightning strike probability, x_e (the distance between the position of the center of the strike location ellipse and the position of the target area) is calculated using the Haversine distance formula.

The collision or strike probability calculation is greatly simplified by reducing the integration over the target area to an integration about a contour enclosing the area. This is achieved by performing a rotation followed by a scale change in the collision or strike plane (Patera 2001, Chan 2008).

Now the probability ellipses of constant pdf (Chan 2008)

$$\frac{x'^2}{\sigma_{x'}^2} + \frac{z'^2}{\sigma_{z'}^2} = k^2 \quad (9)$$

are transformed into circles of constant pdf (Chan 2008)

$$\frac{x''^2}{\sigma_{z'}^2} + \frac{z''^2}{\sigma_{z'}^2} = k^2 \quad (10)$$

where

$$x'' = \frac{\sigma_{z'}}{\sigma_{x'}} x', z'' = z' \quad (11)$$

This transformation circularizes the probability ellipse and turns the target circle into an ellipse. The probability circle is integrated over the target ellipse by means of a contour integral involving only a scalar exponential in the integrand such that (Patera 2001)

$$\begin{aligned} P &= 1 - \frac{1}{2\pi} \sum_0^{1000} e^{-\left(\frac{R}{\sigma_{z'}}\right)^2} d\theta \text{ if } x_e < r_A \\ P &= 1/2 - \frac{1}{2\pi} \sum_0^{1000} e^{-\left(\frac{R}{\sigma_{z'}}\right)^2} d\theta \text{ if } x_e = r_A \\ P &= -\frac{1}{2\pi} \sum_0^{1000} e^{-\left(\frac{R}{\sigma_{z'}}\right)^2} d\theta \text{ if } x_e > r_A \end{aligned} \quad (12)$$

R is calculated by stepping around the target ellipse in increments of $2\pi/1000$. R1 is the distance to the first point on the target ellipse, R2 is the distance to the second incremental point on the target ellipse, and R is the midpoint of vectors R1 and R2. The term $d\theta$ is the angle between R1 and R2, found by taking the cross product of R1 and R2. The integral is evaluated by summing the values of the integrand times $d\theta$ for each pair of points around the ellipse. The minus sign is introduced to be consistent with integrating around the contour in the counter clockwise direction (Patera 2001). The schematic showing this transformation is shown in Figure 2.

c. The second numerical integration technique (Chan, 2011)

The second numerical integration technique is one in which the miss distance is given by a non-central chi distribution with unequal variances. (Chan, 2011) The probability is given by (Chan, 2011)

$$P = \frac{1}{2\sqrt{2\pi}\sigma_H} \int_0^{\sqrt{W}} \left[e^{-(H-\mu_H)^2/2\sigma_H^2} + e^{-(H+\mu_H)^2/2\sigma_H^2} \right] \left[\text{erf}(Z_1) + \text{erf}(Z_2) \right] dH \quad (13)$$

where

$$\begin{aligned} Z_1 &= \left[\sqrt{(W - H^2)} - \mu_K \right] / \sqrt{2}\sigma_K \\ Z_2 &= \left[\sqrt{(W - H^2)} + \mu_K \right] / \sqrt{2}\sigma_K \end{aligned} \quad (14)$$

The parameters μ_K and μ_H are the coordinates of the target circle in the (X', Z') coordinate system; and σ_K and σ_H are the standard deviations of the diagonalized covariance ellipse shown in Equation (4). The derivation of equations (13) and (14) above is shown in further detail in Chan (2011). A detailed example of the calculations using a real-world case is provided in Appendix-A.

3. Evaluation

The probability that any lightning strike is within any radius of any point of interest would be extremely difficult to estimate intuitively. As a result, given the high impact of the decisions on space launch operations, the tool developed for this application was extensively tested. Three major types of tests were conducted and are discussed in the following sections: 1) known mathematical solutions, 2) expected behavior as single

parameters are varied, and 3) examination of real-world events. The new technique passed all of the tests.

a. Test Set 1

The first set of testing compared the lightning strike probability calculated using the 45WS lightning strike spreadsheet (which uses an adaptation of the numerical integration algorithm by Chan (2011)) to the corresponding circular probability from the CRC Handbook of Tables for Probability and Statistics. (Beyer *ed.* 1968) Table 1 shows the probability from the new numerical integration technique for various inputs and the corresponding correct probability from the CRC Handbook. The values matched to within a tenth of a percent. These differences in the final digit may be due to round-off error.

b. Test Set 2

The second set of tests involved verifying that both of the algorithms, the numerical integration techniques, after adaptation into the 45WS spreadsheet, calculated the correct probability. These techniques will be referred to as Patera and Chan, respectively. This involved plotting the calculated probabilities as particular inputs were varied while holding the other inputs constant and comparing results. The results are shown in Figures 3 through 7. The data used to generate these figures are in Table 2. Note that results using both techniques match almost exactly regardless of integration method used. Probability calculations are much faster using Chan's (2011) integration technique as opposed to the numerical integration technique of Patera, 2001.

Figure 3 shows the change in probability as a result of changing the radius around the point of interest while holding all other parameters constant. Chan's method of calculating probability, as well as Patera's method of calculating probability are compared. Both techniques match to the fifth decimal place at all radii.

Figure 4 shows the change in probability as a result of changing the latitude of the strike from the point of interest while holding all other parameters constant. Chan's method and Patera's method of calculating probability are compared. The probability follows a Gaussian curve and reaches a maximum when the uncertainty ellipse is at its closest point of approach to the point of interest, as expected. The probability methods match to the fourth decimal place at all latitudes.

Figure 5 shows the change in probability as a result of changing the longitude of the strike from the point of interest while holding all other parameters constant. Again, both methods are compared. The probabilities follow a Gaussian curve and reach a maximum when the uncertainty ellipse is at its closest point of approach to the point of interest, as expected. The probability methods match to the fourth decimal place at all longitudes.

Figure 6 shows the change in probability as a result of changing the heading from true north of the semi-major axis of the lightning uncertainty ellipse while holding all other parameters constant. Both methods are compared. The center of the stroke uncertainty ellipse is located about 0.5 nautical miles away from the point of interest. The probabilities show a roughly sinusoidal pattern as more, then less, then more of the ellipse rotates into, out of, and back into the area around the point of interest. The probability methods match to the third decimal place at all angles.

Figure 7 shows the change in probability as a result of varying the aspect ratio (length of semi-major axis/length of semi-minor axis) of the lightning uncertainty ellipse from 1.5 to 11 with the strike point close to the point of interest while holding all other parameters constant. Both methods are compared. The probability becomes less as the aspect ratio of the uncertainty ellipse is larger. However, the difference in probability between the two integration techniques is enhanced as the aspect ratio is increased. The probability methods match to the fourth decimal place at all aspect ratios.

In light of the similarity of results between calculation methods, the 45WS decided to use Chan's (2011) numerical integration technique to calculate probabilities. The program run time is a minimum of two times faster using Chan's numerical integration technique and since 45WS must sometimes process thousands of lightning strokes after intense local lightning events, it was advantageous to use the algorithm with the faster run time given equivalent accuracy.

c. Test Set 3

The third type of testing analyzed six real-world lightning strikes near Space Launch Complex 39A on 3 August 2009. Figure 8 shows the spreadsheet used to generate the lightning report for those six strikes. Additional data on these strikes are in Table 3. These strikes were selected because the closest point on the lightning position uncertainty ellipse was within 0.45 nautical miles of Launch Complex 39A, the key radius for assessing the need to inspect electronics for induced current damage to the Space Shuttle. Figures 9 through 11 are Google Maps depictions of three of these six strokes. The probabilities for a small area around a facility, even for a nearby stroke,

may appear to be surprisingly low. For example, one strike just 0.65 nautical miles away (Figure 9) had only a 1.1% probability of being within the 0.45 nautical mile radius of Launch Complex 39A. All calculated probabilities are consistent with these real-world events.

The KSC Electromagnetic Environmental Effects (EEE) Panel requested six more real-world lightning strikes be investigated. These were recently investigated lightning strikes near Launch Complexes 39A or 39B where there was camera verification of the location of the strike. The EEE Panel wanted to compare the results of the new facility-centric probabilistic technique to these cases where the true answers were known unambiguously. The data used for this analysis are in Table 4. Both 4DLSS and National Lightning Data Network (NLDN) cases were examined, depending upon which sensor system recorded the stroke. CGLSS strokes were obtained from 45WS 4DLSS. The NLDN usually provided flash data, so NLDN return stroke data were purchased as special StrikeNet reports from Vaisala Corporation (Vaisala, 2006). This was done to match the return strokes routinely provided by 4DLSS. Figures 12 through 14 show the probability results from these cases. As with the previous real-world tests, all calculated probabilities were consistent with these additional real-world events.

4. Summary

A technique has been developed to calculate the probability that any nearby cloud-to-ground lightning stroke occurred within any radius of any point of interest. In practice, this provides the probability that a nearby lightning stroke was within a key distance of a facility, rather than within the error ellipses centered on the stroke. This

process uses the bivariate Gaussian distribution of probability density provided by the current lightning location error ellipse for the most likely location of a lightning stroke and integrates it to determine the probability that the stroke is inside any specified radius. This new facility-centric technique which was tested extensively, is much more useful to the space launch customers, and will supersede the lightning error ellipse approach discussed in Flinn et al 2010a, Flinn et al 2010b.

The techniques and methods described in this paper clearly have application reaching far beyond the space program uses for which it was designed. The list of potential applications is many and varied and would be of interest to anyone seeking information pertaining to probability of lightning strike locations, such as the power industry, aviation, or any industry sensitive to electrical overloads. This methodology is also applicable to forensic meteorology (see, e.g., Austin, 2010) where the question of whether lightning struck at or near a particular location is an issue in litigation.

Acknowledgments.

This work would not exist were it not for the generous contributions and suggestions by Dr. Ken Chan of the Aerospace Corp, who is an expert on spacecraft collision probability, on whose work the probability of lightning within a radius of interest was based. Dr. Darrin Leleux of the Johnson Space Center, Houston, TX, and Dr. Walt Gill of Sandia National Laboratory also provided helpful guidance and testing. Mr. Jeremy Hinkley and Mr. Pete Hopman of United Space Alliance, the prime contractor for Space Shuttle operations, provided very valuable efficiency modifications

for the visual basic code and also integrated the probability calculations and closest ellipse point algorithm into the 45th Weather Squadron Lightning Report Spreadsheet. The authors appreciate a helpful review of an earlier draft of this paper by Mr. John Madura of the Kennedy Space Center. This work was done under the Kennedy Space Center Employee Development Program.

APPENDIX A

Probability calculation example for a lightning strike

This appendix is an example of calculating the probability of any lightning stroke with a known error ellipse being within a circle of any radius around any point. It is provided to clarify the calculation process. An example calculation is shown in Table A-1.

This example is a real-world event from a lightning strike near the Space Shuttle launch pad 39A at 21:30 GMT on 14 Oct 2009 (ref. Figure 12). Although the lightning data usually are from the cloud-to-ground component of the Four Dimensional Lightning Surveillance System (CG-4DLSS) (Murphy et al 2008, Roeder 2010) in this example a lightning stroke from the NLDN is used. We sometimes use StrikeNet reports that provide stroke data from the NLDN to double check the CG-4DLSS report.

- Location of Launch Pad 39A: 28.60827486 N (or 0.499309 radians)
-80.60411653 (i.e. 80.60411653 W or -1.406807 radians) This is also the center of the circle in which the lightning probability will be calculated.
- Desired Radius For Probability of Lightning Around 39A: 0.45 nautical miles

- Lightning Stroke Data: Time/Date: 0235 GMT, 16 Aug 2009

Latitude: 28.6069 N (or 0.499285 radians)

Longitude: -80.6087 (i.e. 80.6087 W or -1.406887 radians)

Polarity/Peak Current: -43.0 kA

Semi-major axis of 50% confidence location ellipse: 0.6 km

Semi-minor axis of 50% confidence location ellipse: 0.4 km

Orientation angle of location ellipse: 82° (clockwise from north)

References

Alfano, S., 2007: "Review of Conjunction Probability Methods for Short-term Encounters" AAS Paper No. 07-148, *AAS/AIAA Space Flight Mechanics Meeting*, Sedona, Arizona, 28 January-01 February 2007.

Alfano, S., 2009: "Satellite Collision Probability Enhancements" *J. Guidance, Control, and Dynamics*, **29**(3), 588-592.

Austin, E., 2010: Forensic Meteorology & Climatology: A rapidly emerging niche, Paper 1.2, Third Annual CCM Forum, 90th Annual AMS Meeting, Atlanta, GA, 16 – 21 January, 2010.

Chan, F. Kenneth, 2008. *Spacecraft Collision Probability*. The Aerospace Press, El Segundo, CA.

Chan, F. Kenneth, 2011: “Miss Distance – Generalized Variance Non-Central Chi Distribution.” Paper accepted for the AAS/AIAA Space Flight Mechanics Meeting in New Orleans February 13-17, 2011.

CRC Handbook of Tables for Probability and Statistics, 2nd edition, 1968: W. H. Beyer, editor, Cleveland, OH: The Chemical Rubber Co., 151-157.

Flinn, F. C., W. P. Roeder, M. D. Buchanan, and T. M. McNamara, 2010a: Lightning Reporting at 45th Weather Squadron: Recent Improvements, *21st International Lightning Detection Conference*, 19-20 Apr 10, 18 pp..

Flinn, F. C., W. P. Roeder, D. F. Pinter, S. M. Holmquist, M. D. Buchanan, T. M. McNamara, M. McAleenan, K. A. Winters, P. S. Gemmer, M. E. Fitzpatrick, and R. D. Gonzalez, 2010b: Recent Improvements in Lightning Reporting At 45th Weather Squadron, *14th Conference on Aviation, Range, and Aerospace Meteorology*, 17-21 Jan 10, Paper 7.3, 14 pp.

Leleux, D., et. al., 2002: Probability-based Space Shuttle collision avoidance, *Space Ops 2002 Conference*, 20-24 Oct 2002, 18 pp.

Murphy, M. J., K. L. Cummins, N. W. S. Demetriades, and W. P. Roeder, 2008: Performance Of The New Four-Dimensional Lightning Surveillance System (4DLSS) At

The Kennedy Space Center/Cape Canaveral Air Force Station Complex, *13th Conference on Aviation, Range, and Aerospace Meteorology*, 20-24 Jan 07, 18 pp.

Patera, Russell. P., 2001: "General Method for Calculating Satellite Collision Probability" *J. Guidance, Control, and Dynamics*, **24**(4), 716-722.

Roeder, W. P., 2010: The Four Dimension Lightning Surveillance System. *21st International Lightning Detection Conference*, 21-22 Apr 10, 15 pp.

Roeder, W. P., J. W. Weems, and P. B. Wahner, 2005: Applications of the Cloud-To-Ground-Lightning-Surveillance-System Database. *1st Conference on Meteorological Applications of Lightning Data*, 9-13 Jan 05, 5 pp.

Vaisala, 2006: Vaisala StrikeNet information, *Vaisala, Inc*, www.vaisala.com/files/StrikeNet-Brochure.pdf, 2006, 6 pp.

List of Figures

FIG. 1. Schematic diagram of the angles used in probability calculation for a sample lightning location error ellipse. α is the heading of the semi-major axis of the lightning location uncertainty ellipse from true north. θ is the angle between the semi-major axis of the lightning location uncertainty ellipse and line connecting the center of the lightning uncertainty ellipse and the center of the area of interest.

FIG. 2. Schematic diagram describing the conversion of the bivariate Gaussian pdf lightning location error ellipse into a probability circle and the target area of interest into an ellipse. (Adapted from Chan, 2008.)

FIG. 3. Change in probability as a result of changing the point of interest radius while holding all other parameters constant.

FIG. 4. Change in probability as a result of changing the latitude of the strike from the point of interest while holding all other parameters constant.

FIG. 5. Change in probability as a result of changing the longitude of the strike from the point of interest while holding all other parameters constant.

FIG. 6. Change in probability as a result of changing the semi-major axis heading of the lightning uncertainty ellipse while holding all other parameters constant.

FIG. 7. Change in probability as a result of varying the aspect ratio (length of semi-major axis/length of semi-minor axis) of the lightning uncertainty ellipse from 1.5 to 11 with the strike point close to the point of interest while holding all other parameters constant.

FIG. 8. Sample of lightning strikes where the closest point on the lightning position uncertainty ellipse was within 0.45 nmi of Launch Complex 39A on 3 August 2009.

FIG. 9. Google Maps visualization of the 99% confidence uncertainty ellipse for one of the closest lightning strikes to Complex 39A on 03 August 2009. The center of the ellipse was within the 0.45 nmi radius. There is a 53.8% probability that the lightning occurred within that radius.

FIG. 10. Google Maps visualization of the 99% confidence uncertainty ellipse for nearby lightning strike to Complex 39A on 03 August 2009. Figure 10 shows a probability of 7.7% of the lightning strike occurring within the 0.45 nmi radius.

FIG. 11. Google Maps visualization of the 99% confidence uncertainty ellipse for nearby lightning strike to Complex 39A on 03 August 2009. Figure 11 shows a probability of 1.1% of the lightning strike occurring within the 0.45 nmi radius.

FIG. 12. Illustrates a probability of 69.1% of a lightning strike of amplitude -43.0 kA detected by NLDN occurring 0.26 nmi from the center of Launch Complex 39A on 8/16/2009.

FIG. 13. Illustrates a probability of 74.7% of a lightning strike of amplitude -71.4 kA detected by NLDN occurring 0.28 nautical miles from the center of Launch Complex 39A on 10/14/2009.

FIG. 14. Illustrates a probability of 99.9996% of a lightning strike of amplitude -21.7 kA detected by CGLSS occurring 0.04 nmi from the center of Launch Complex 39B on 6/27/2009.

TABLE 1. Calculated probability vs. CRC Handbook probability for various inputs.

Semi-major Axis (nmi)	Semi-minor Axis (nmi)	Heading of semi-major axis from true North	Point Of Interest latitude	Point Of Interest longitude	Strike Latitude	Strike Longitude	Radius around Point Of Interest (nmi)	Calculated probability	CRC Handbook probability [4]
3	3	15	28.6082	-80.6041	28.6995	-80.6041	3	0.095	0.095
3	3	15	28.6082	-80.6041	28.631	-80.6041	3	0.453	0.452
3	3	15	28.6082	-80.6041	28.608	-80.6041	3	0.500	0.499
1	1	15	28.6082	-80.6041	28.608	-80.6041	1	0.500	0.499
1	1	15	28.6082	-80.6041	28.631	-80.6041	1	0.200	0.200
1	1	15	28.6082	-80.6041	28.6995	-80.6041	1	0.000	0.000
1	1	15	28.6082	-80.6041	28.608	-80.6041	2	0.937	0.938

TABLE 2. Input values used for scenarios shown in Figures 3 through 7.

Figure	Semi-major axis of 50% Confidence Ellipse (km)	Semi-minor axis of 50% Confidence Ellipse (km)	Confidence	Heading (from true North) of semi-major axis	Point Of Interest latitude (°N)	Point Of Interest longitude (°W)	Strike latitude (°N)	Strike longitude (°W)	Radius around Point Of Interest (nmi)
3	3.1	1.2	0.50	75	28.60827	80.6041	28.59	80.59	Varied
4	0.3	0.2	0.50	44.3	28.60827	80.6041	Varied	80.6041	0.45
5	0.3	0.2	0.50	44.3	28.60827	80.6041	28.6082	Varied	0.45
6	0.3	0.2	0.50	Varied	28.60827	80.6041	28.6162	80.6041	0.45
7	Varied	0.12	0.50	90	28.60827	80.6041	28.6062	80.6041	0.45

TABLE 3. Input values used for scenarios shown in Figures 9 through 11.

Figure	Semi-major axis of 50% Confidence Ellipse (km)	Semi-minor axis of 50% Confidence Ellipse (km)	Confidence	Heading (from true North) of semi-major axis	Point Of Interest latitude (°N)	Point Of Interest longitude (°W)	Strike latitude (°N)	Strike longitude (°W)	Radius around Point Of Interest (nmi)
9	0.4	0.2	0.99	300.7	28.60827	80.6041	28.6114	80.6113	0.45
10	0.3	0.2	0.99	293	28.60827	80.6041	28.6178	80.6069	0.45
11	0.2	0.1	0.99	20.3	28.60827	80.6041	28.5995	80.6113	0.45

TABLE 4. Input values used for scenarios shown in Figures 12 through 14.

Figure	Semi-major axis of 50% Confidence Ellipse (km)	Semi-minor axis of 50% Confidence Ellipse (km)	Confidence	Heading (from true North) of semi-major axis	Point Of Interest latitude (°N)	Point Of Interest longitude (°W)	Strike latitude (°N)	Strike longitude (°W)	Radius around Point Of Interest (nmi)
12	0.6	0.4	0.99	82	28.60827	80.6041	28.6069	80.6087	0.45
13	0.4	0.4	0.99	95	28.60827	80.6041	28.6057	80.6085	0.45
14	0.2	0.1	0.99	72	28.62716	80.6208	28.6275	80.6202	0.45

Table A-1. Lightning strike probability calculation process

STEP	ACTION	EQUATION & OTHER INFORMATION	CALCULATION & RESULT
1	Convert semi-major and semi-minor axes from km to nmi	1 nmi = 1.852 km	0.6 km = 0.324 nmi semi-major axis 0.4 km = 0.216 nmi semi-minor axis
2	Calculate distance from lightning stroke to center of circle	<p>Haversine Distance Formula: Distance = Earth Radius * C</p> <ul style="list-style-type: none"> Earth Radius = 3443.920086 nmi $C = 2 * \text{Atn2}[\sqrt{1-A}, \sqrt{A}]$ <p>Atn2 is a two parameter arc tangent function which returns values in all four quadrants.</p> <ul style="list-style-type: none"> $A = \sin(\text{dlat}/2) * \sin(\text{dlat}/2) + \cos(\text{target lat}) * \cos(\text{stroke lat}) * \sin(\text{dlon}/2) * \sin(\text{dlon}/2)$ dlat = latitude difference from target to stroke = $28.60827^\circ - 28.6069^\circ = 2.39959 \times 10^{-5}$ (radians) dlon = longitude difference from circle to stroke = - $80.60411^\circ - 80.6085^\circ = 7.99967 \times 10^{-5}$ (radians) 	<p>Distance = $3443.920086 * 7.4217 \times 10^{-5} = 0.2556$ nmi</p> <p>$C = 2 * \text{Atn2}\{\text{sqr}(1 - 1.377 \times 10^{-9}), \text{sqr}(1.377 \times 10^{-9})\} = 7.4217 \times 10^{-5}$</p> <p>$A = \sin(1.200 \times 10^{-5}/2) * \sin(1.200 \times 10^{-5}/2) + \cos(0.4993) * \cos(0.4993) * \sin(4.000 \times 10^{-5}/2) * \sin(4.000 \times 10^{-5}/2) = 1.3770 \times 10^{-9}$</p>
3	Perform coordinate system rotation to eliminate the off-diagonal term in the covariance matrix.	<ul style="list-style-type: none"> $X = (\text{Longitude of Target} - \text{Longitude of Stroke}) * \cos(\text{Latitude of Strike})$ $Z = \text{Latitude of Target} - \text{Latitude of Stroke}$ $\theta = \alpha - ((\pi/2) - \text{Atn2}(X, Z))$ α is the orientation angle of the 50% lightning positional confidence ellipse $X' = \text{miss distance} * \cos(\theta \text{ (coordinate system rotation angle)})$ $Z' = \text{miss distance} * \sin(\theta)$ 	<p>$X = (-1.4068 - (-1.4069)) * \cos(0.4993) = 7.0231 \times 10^{-5}$</p> <p>$Z = 0.49931 - 0.49929 = 2.400 \times 10^{-5}$</p> <p>$\theta = 1.431 - 1.571 - \text{Atn2}(7.023 \times 10^{-5}, 2.400 \times 10^{-5}) = 0.1896$</p> <p>$X' = 0.2556 * \cos(0.1896) = 0.2510$</p> <p>$Z' = 0.2556 * \sin(0.1896) = 0.0482$</p>
4	Calculate	<ul style="list-style-type: none"> $\sigma_{X'} = \text{Semi-major axis of the 50\%}$ 	$k = \sqrt{-2 * \ln(1 - 0.50)} =$

	the standard deviations in the new rotated coordinate system.	<p>lightning positional confidence ellipse /elliptical scaling constant used to scale standard error to the 50% confidence level</p> <ul style="list-style-type: none"> • $\sigma_{Z'}$ = Semi-minor axis of the 50% lightning positional confidence ellipse /elliptical scaling constant used to scale standard error to the 50% confidence level • Elliptical scaling constant, k, is: $\sqrt{-2 * \ln(1 - probability)}$ 	<p>1.1774</p> $\sigma_{X'} = 0.3240 / 1.1774 = 0.2752$ $\sigma_{Z'} = 0.2160 / 1.1774 = 0.1834$
5	Calculate the probability that lightning stroke was within the target area of interest by performing a numerical integration using Simpson's rule of the lightning uncertainty ellipse over the area of the circle around the target of interest.	$P = \frac{1}{2\sqrt{2\pi}\sigma_H} \int_0^{\sqrt{W}} \left[e^{-(H-\mu_H)^2/2\sigma_H^2} + e^{-(H+\mu_H)^2/2\sigma_H^2} \right] [erf(Z_1) + erf(Z_2)] dH$ $Z_1 = \left[\sqrt{(W-H^2)} - \mu_K \right] / \sqrt{2}\sigma_K$ $Z_2 = \left[\sqrt{(W-H^2)} + \mu_K \right] / \sqrt{2}\sigma_K$ <ul style="list-style-type: none"> • μ_K and μ_H are the coordinates of the target circle in the (X', Z') coordinate system • σ_K and σ_H are equal to $\sigma_{X'}$ and $\sigma_{Z'}$ which are the standard deviations of the diagonalized covariance matrix. • W = Radius around target² • N = the number of iterations to perform in the integration (for this example, N is set to 200). • $DH = \sqrt{W} / N$ = integration step • B, C, and D are intermediate variables in the algorithm corresponding to various parts of the probability equation shown above <ul style="list-style-type: none"> • $B = \sqrt{2} * \sigma_{X'}$ • $C = X' / B$ • $D = 1 / (2 * \sqrt{2\pi} * \sigma_{Z'})$ • A, H, z1, z2, E, F, Erf(z1), Erf(z2), Q and sum are intermediate variables in the algorithm corresponding to various parts of the probability equation shown above • A loop is performed for j = 1 to 199. This example is shown for j = 199. 	<p>W = Radius around target²</p> $W = 0.45^2 = 0.2025$ <p>$DH = \sqrt{W} / N$</p> $DH = \sqrt{0.2025} / 200 = 0.00225$ <p>$B = \sqrt{2} * \sigma_{X'}$</p> $B = \sqrt{2} * 0.2752 = 0.3891$ <p>$C = X' / B$</p> $C = 0.2510 / 0.3891 = 0.6451$ <p>$D = 1 / (2 * \sqrt{2\pi} * \sigma_{Z'})$</p> $D = 1 / (2 * \sqrt{2\pi} * 0.1834) = 1.0874$ <p>H = iteration no. * DH</p> $H = 199 * 0.00225$ $H = 0.4478$ <p>$A = \sqrt{W - H^2}$</p> $A = \sqrt{0.2025 - 0.44775^2}$ $A = 4.494 \times 10^{-2}$ <p>$z1 = A / B - C$</p> $z1 = 4.494 \times 10^{-2} / 0.3891 - 0.6451$ $z1 = -0.5296$ <p>$z2 = A / B + C$</p> $z2 = 4.494 \times 10^{-2} / 0.3891$

		<ul style="list-style-type: none"> • Sum = 0 • Begin Loop here: $H = j * DH$ • $A = \sqrt{W - H^2}$ • $z1 = A/B - C$ • $z2 = A/B + C$ • $\text{Erf}(x) = \text{error function} = \frac{2}{\sqrt{\pi}} \int_0^x e^{-t^2} dt$ • $E = (H - Z')^2 / (2 * \sigma_Z'^2)$ • $F = (H + Z')^2 / (2 * \sigma_Z'^2)$ • $Q(j) = (e^{-E} + e^{-F}) * (\text{Erf}(Z1) + \text{Erf}(Z2))$ • $\text{sum} = \text{sum} + (3 - (-1)^j) * Q(j)$ <ul style="list-style-type: none"> • $\text{sum} = \text{sum} + Q(0) + Q(N)$ • $\text{Probability} = D * \text{sum} * DH / 3$ 	<p>+ 0.6451 $z2 = 0.7606$</p> <p>$\text{Erf}(Z1) =$ $\text{ErrorFunction}(z1)$ $\text{Erf}(-0.5296) = -0.5461$</p> <p>$\text{Erf}(Z2) =$ $\text{ErrorFunction}(z2)$ $\text{Erf}(0.7606) = 0.7179$</p> <p>$E = (H - Z')^2 / (2 * \sigma_Z'^2)$ $E = (0.4478 - 0.0482)^2 / (2 * 0.1834^2)$ $E = 2.372$ $F = (H + Z')^2 / (2 * \sigma_Z'^2)$ $F = (0.4478 + 0.0482)^2 / (2 * 0.1834^2)$ $F = 3.654$</p> <p>$Q(j) = (e^{-E} + e^{-F}) * (\text{Erf}(Z1) + \text{Erf}(Z2))$ $Q(199) = (e^{-2.372} + e^{-3.654}) * (-0.5461 + 0.7179) = 2.0467 \times 10^{-2}$</p> <p>$\text{sum} = \text{sum} + (3 - (-1)^j) * Q(j)$ $\text{sum} = \text{sum} + (3 - (-1)^{199}) * 2.047 \times 10^{-2}$ $\text{sum} = 844.8952$ End Loop</p> <p>$\text{sum} = \text{sum} + Q(0) + Q(N)$ $\text{sum} = 844.8952 + 2.9361 + 0 = 847.8317$</p> <p>$\text{Probability} = D * \text{sum} * DH / 3$ $\text{Probability} = 1.0874 * 847.8317 * 0.00225 / 3 = 0.6914$</p>
--	--	---	---

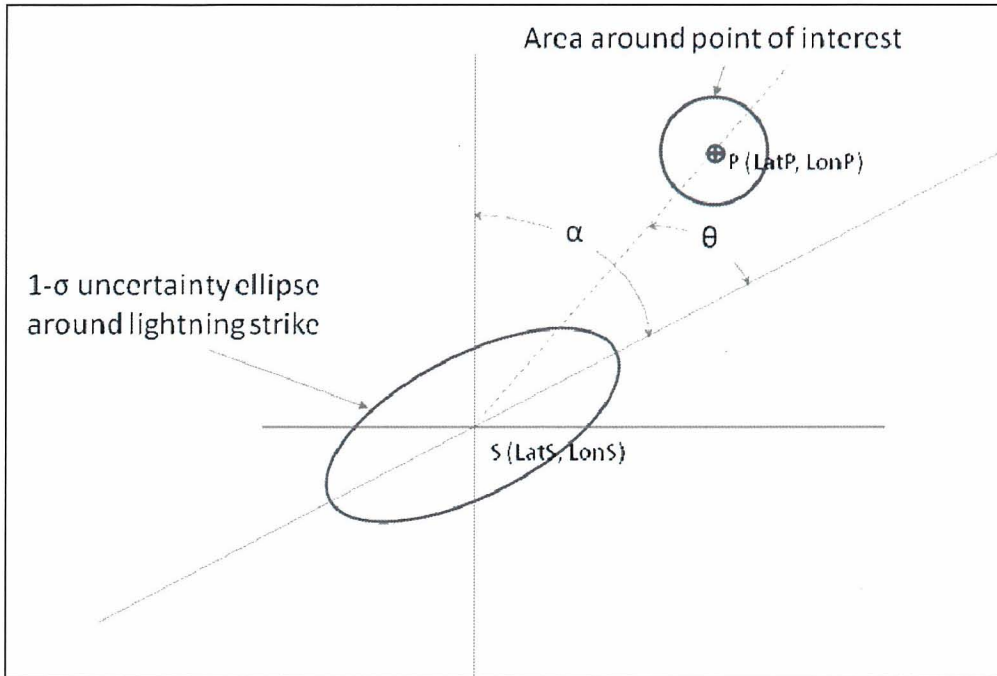


FIG. 1. Schematic diagram of the angles used in probability calculation for a sample lightning location error ellipse. α is the heading of the semi-major axis of the lightning location uncertainty ellipse from true north. θ is the angle between the semi-major axis of the lightning location uncertainty ellipse and line connecting the center of the lightning uncertainty ellipse and the center of the area of interest.

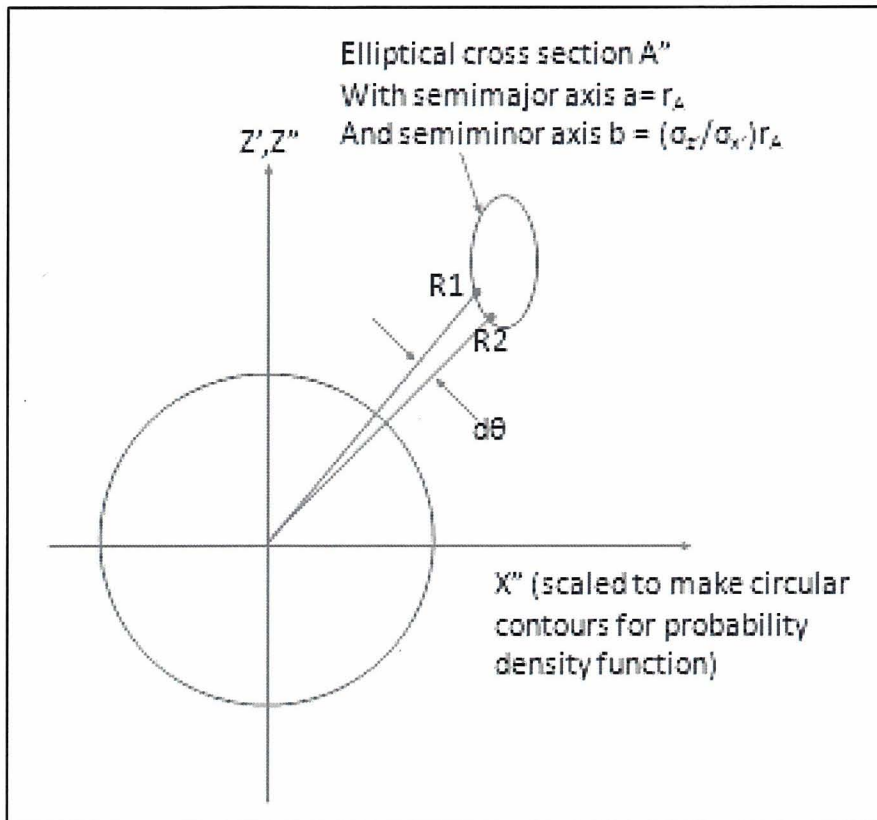


FIG. 2. Schematic diagram describing the conversion of the bivariate Gaussian pdf lightning location error ellipse into a probability circle and the target area of interest into an ellipse. (Adapted from Chan, 2008.)

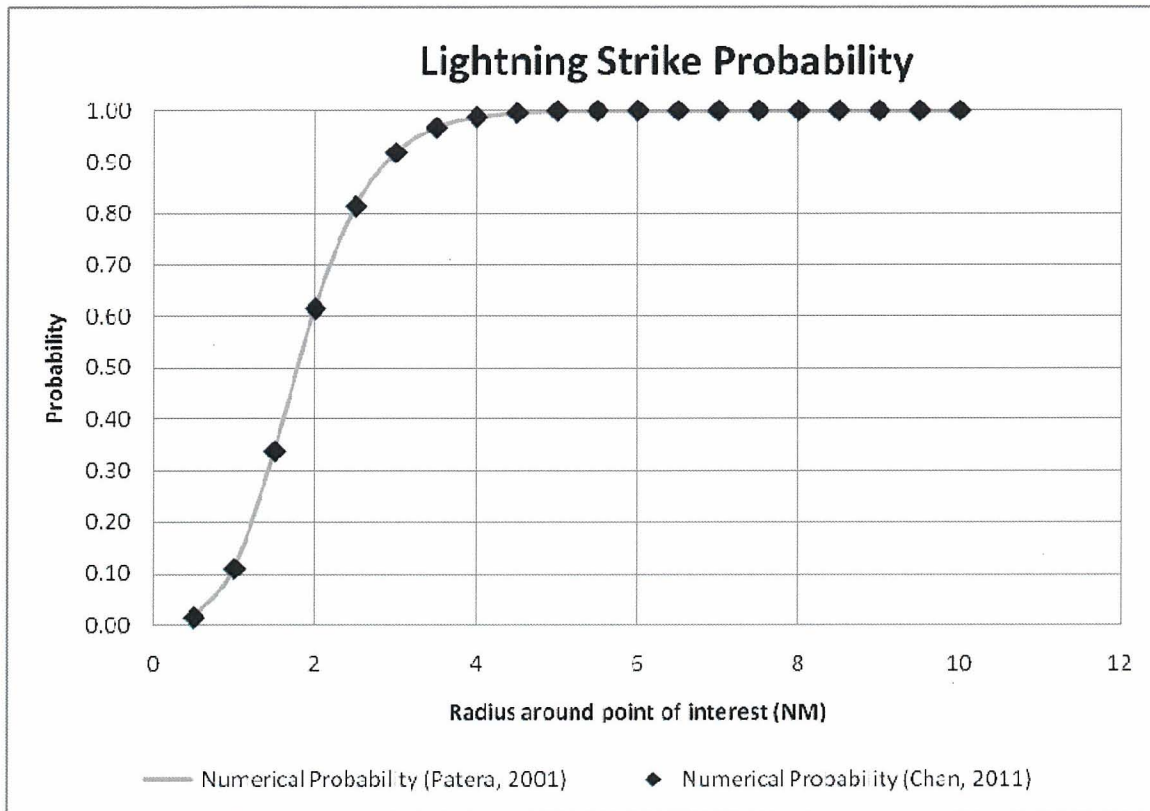


FIG. 3. Change in probability as a result of changing the point of interest radius while holding all other parameters constant.

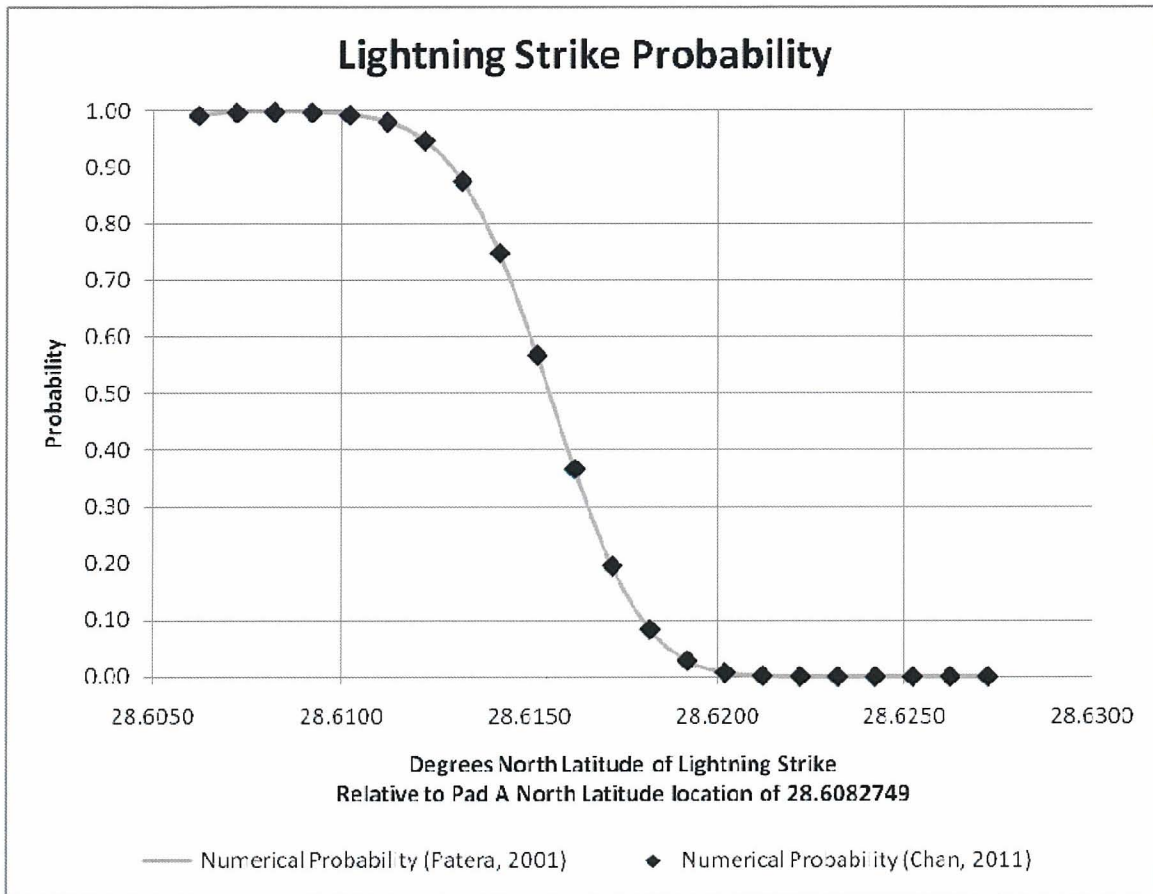


FIG. 4. Change in probability as a result of changing the latitude of the strike from the point of interest while holding all other parameters constant.

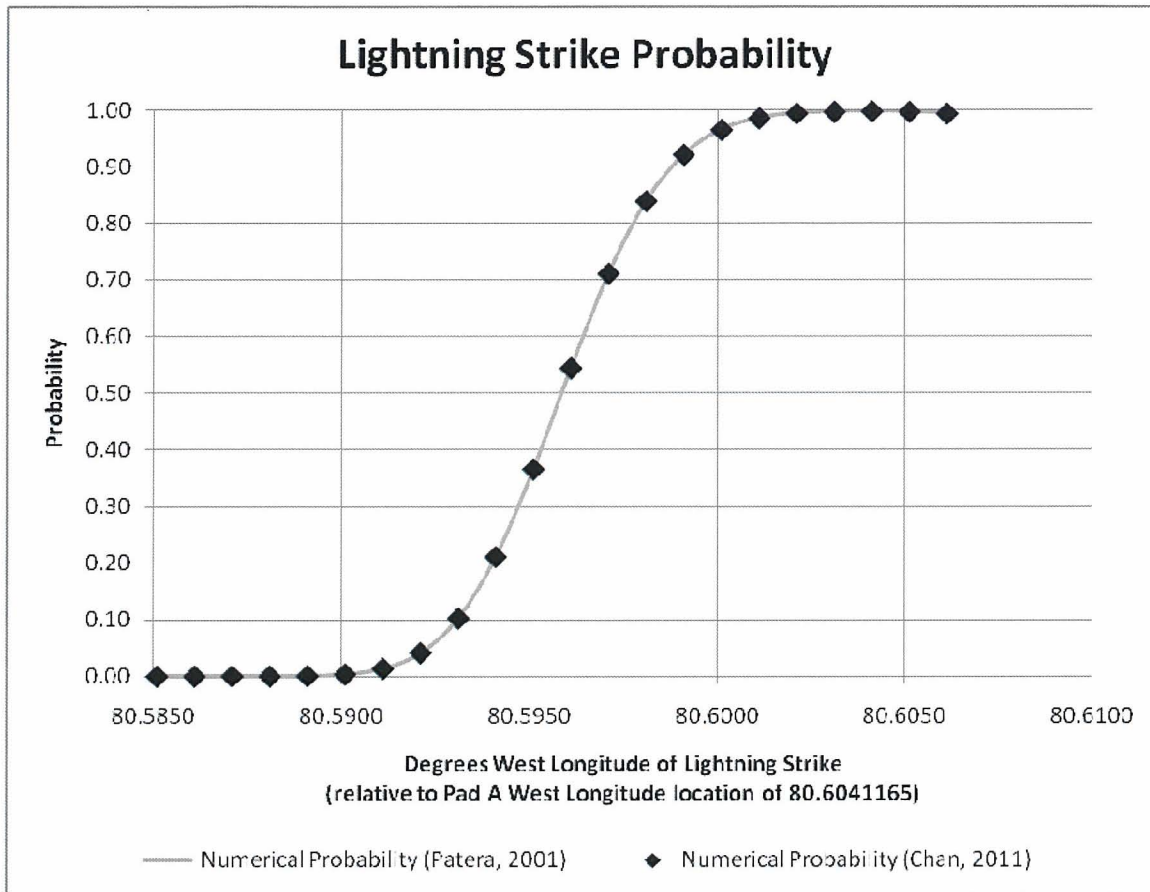


FIG. 5. Change in probability as a result of changing the longitude of the strike from the point of interest while holding all other parameters constant.

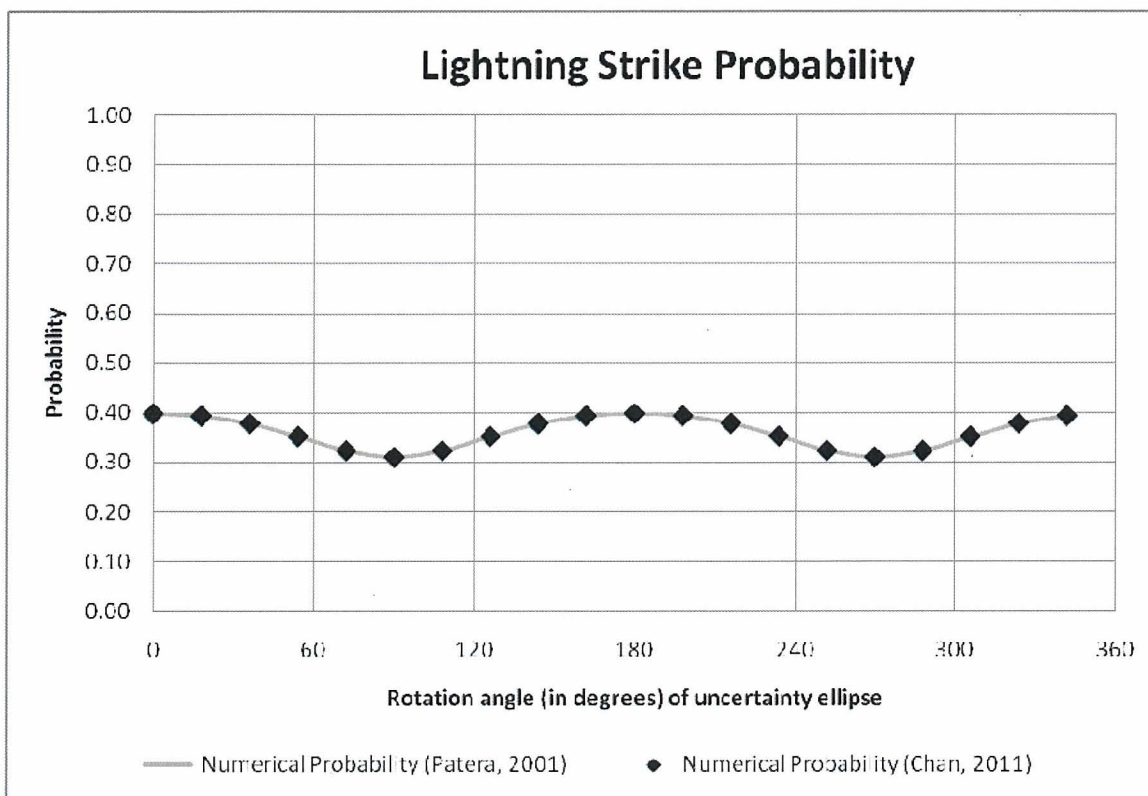


FIG. 6. Change in probability as a result of changing the semi-major axis heading of the lightning uncertainty ellipse while holding all other parameters constant.

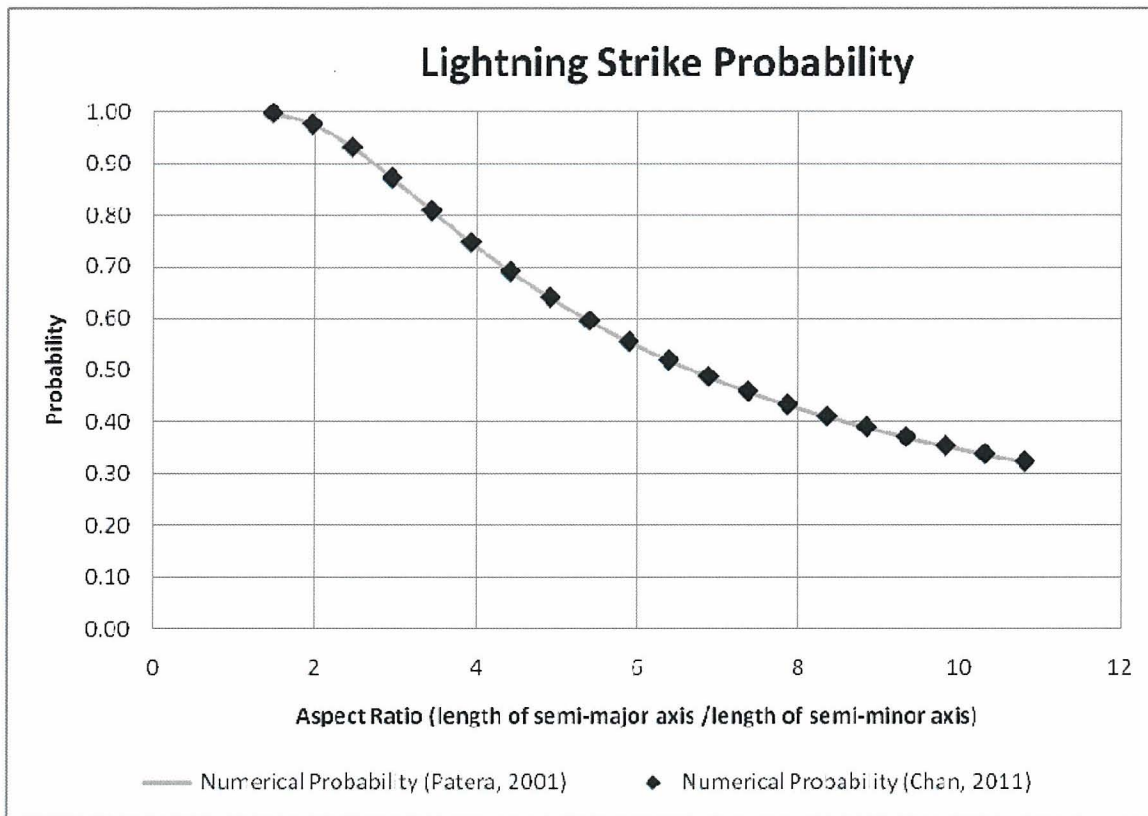


FIG. 7. Change in probability as a result of varying the aspect ratio (length of semi-major axis/length of semi-minor axis) of the lightning uncertainty ellipse from 1.5 to 11 with the strike point close to the point of interest while holding all other parameters constant.

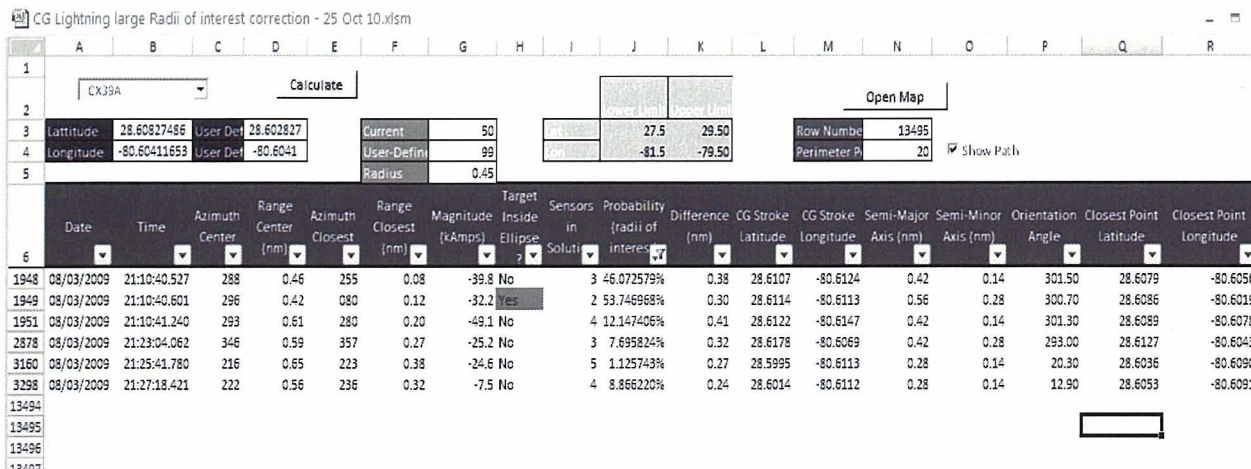


FIG. 8. Sample of lightning strikes where the closest point on the lightning position uncertainty ellipse was within 0.45 nmi of Launch Complex 39A on 3 August 2009.



FIG. 9. Google Maps visualization of the 99% confidence uncertainty ellipse for one of the closest lightning strikes to Complex 39A on 03 August 2009. The center of the ellipse was within the 0.45 nmi radius. There is a 53.8% probability that the lightning occurred within that radius.

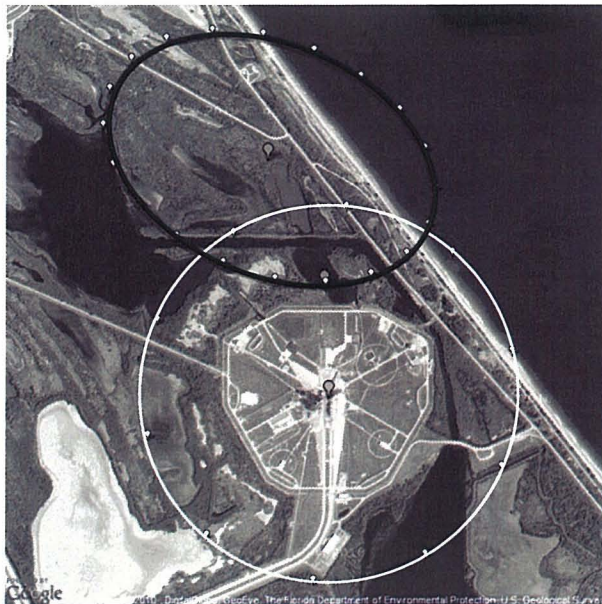


FIG. 10. Google Maps visualization of the 99% confidence uncertainty ellipse for a lightning strike near Complex 39A on 03 August 2009. Figure 10 shows a probability of 7.7% of the lightning strike occurring within the 0.45 nmi radius.



FIG. 11. Google Maps visualization of the 99% confidence uncertainty ellipse for nearby lightning strike to Complex 39A on 03 August 2009. Figure 11 shows a probability of 1.1% of the lightning strike occurring within the 0.45 nmi radius.



FIG. 12. Illustrates a probability of 69.1% of a lightning strike of amplitude -43.0 kA detected by NLDN occurring 0.26 nmi from the center of Launch Complex 39A on 8/16/2009.



FIG. 13. Illustrates a probability of 74.7% of a lightning strike of amplitude -71.4 kA detected by NLDN occurring 0.28 nautical miles from the center of Launch Complex 39A on 10/14/2009.

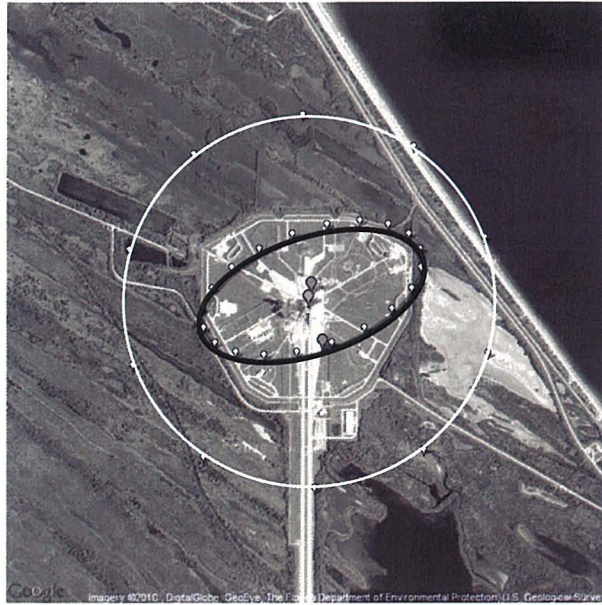


FIG. 14. Illustrates a probability of 99.9996% of a lightning strike of amplitude -21.7 kA detected by CGLSS occurring 0.04 nmi from the center of Launch Complex 39B on 6/27/2009.